

# Temperature-Stabilized and Widely Tunable Vertical External Cavity Surface-Emitting Laser With a Simple Line Cavity

Xiaolang Qiu <sup>1</sup>, Graduate Student Member, IEEE, Chao Wang, Jian Li, Chuanchuan Li, Xinyu Xie, Yongli Wang, and Xin Wei <sup>2</sup>

**Abstract**—We designed and demonstrated a temperature-stable, wide-tuned, high-power Vertical External Cavity Surface-emitting Laser (VECSEL) with a simple linear cavity. The quantum well is optimized by using the commercial PICS3D software to obtain wide gain and good thermal performance. The curve of BF has also been optimized, and a birefringent filter (BF) with a thickness of 1mm is selected as the tuning element. Then, we obtained a continuously adjustable range cover from 1044.5 nm to 1092.1 nm, 8 W of output power, and temperature-stable VECSEL, which verifies the feasibility of the design. Based on the experimental results, we concluded that the gain intensity corresponding to the tuning range should be at least greater than  $163 \text{ e}^{26}/\text{cm}^{-3}\text{s}^{-1}\text{eV}^{-1}$  before the growth process ensures a wide tuning range. For the first time, to the best of our knowledge, we designed and obtained the tuning result of VECSEL in the linear cavity, and this is of great significance to the design of VECSEL with wide-tuning, high-power, and good temperature stability.

**Index Terms**—Semiconductor lasers, diode-pumped lasers, tunable lasers, temperature-stable.

## I. INTRODUCTION

HIGH-POWER, tunable lasers play a significant role in scientific research, industry, and defense applications. The wavelength tuning range is one of the fundamental parameters for lasers to achieve various practical fields, such as environmental monitoring, spectral analysis, coherent measurement, imaging, and monitoring [1]–[5]. Optically Pumped Vertical External Cavity Surface-Emitting Lasers (OP-VECSELs) combine the advantages of semiconductor lasers and solid-state disk lasers, not only with a gain bandwidth of tens of nanometers or more but also with external cavity structure [6], [7]. The flexible external cavity structure of VECSEL allows the insertion of

Manuscript received 8 July 2022; revised 27 July 2022; accepted 28 July 2022. Date of publication 2 August 2022; date of current version 15 August 2022. This work was supported in part by the National Natural Science Foundation of China under Grant 62004190, and in part by the National Key Research and Development Program of China under Grant 2018YFE0203101. (Corresponding author: Xin Wei.)

Xiaolang Qiu, Jian Li, Chuanchuan Li, Xinyu Xie, Yongli Wang, and Xin Wei are with the Nano Optoelectronics Laboratory, Institute of Semiconductors, Chinese Academy of Sciences, Beijing 10083, China, and also with the University of Chinese Academy of Sciences, Beijing 100049, China (e-mail: qiuxiaolang@semi.ac.cn; jalain@semi.ac.cn; lichuan@semi.ac.cn; 1179563288@qq.com; wangyongli@semi.ac.cn; weix@semi.ac.cn).

Chao Wang is with the Academy of Quantum Information Sciences, Beijing 100193, China (e-mail: wangchao@baqis.ac.cn).

Digital Object Identifier 10.1109/JPHOT.2022.3195751

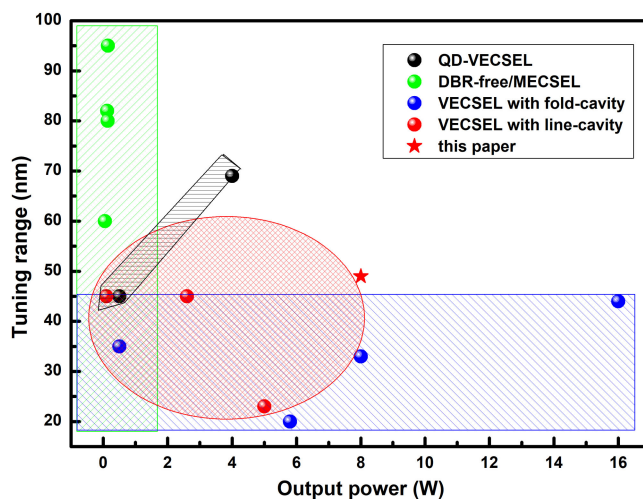


Fig. 1. Comparison of tuning range as a function of output power near  $1 \mu\text{m}$  for VECSEL: the green balls are for DBR-free/MECSELs [17]–[20], the black balls are for quantum dot VECSELs [21], the blue balls are for VECSEL with fold cavity [10], [22]–[24], the red balls are for VECSEL with line-cavity [12], [25], [26], the red star is VECSEL with line-cavity in this paper.

optical elements such as birefringent filters, frequency doubling crystals, saturable absorbers, etc., for frequency doubling [8], dual-wavelength [9], wavelength tuning [10]–[12], and ultra-short pulse [13], [14].

In most applications, for example, optical coherence tomography, frequency metrology, laser spectral absorption, and high-efficiency pump source for Er/Yb co-doped single-mode fiber lasers [15], require stable and adjustable wavelength. Tunable high-power VECSELs are very attractive candidates to meet these applications. The most common approach to tuning VECSEL is to insert a birefringent filter (BF) in the cavity, which not only avoids large insertion loss but also enables wavelength tuning and narrow linewidth [16]. The partial reports of using BF to realize wide tuning VECSEL near  $1 \mu\text{m}$  are shown in Fig. 1.

There are various ways to realize the widely tuning VECSEL. For example, the distributed Bragg Reflector (DBR)-free VECSELs (also known as Membrane External Cavity Surface Emitting Lasers, MECSELs) can achieve a wide tuning range up to 90 nm, but the output power is below 1 W. Moreover, the DBR-free VECSELs require cumbersome resonator structure

design and adjustment, which sacrifices the compactness and integration of VECSELS. The quantum dot (QD) VECSELS can obtain a wide tuning range, but it needs complex epitaxial growth processes and power scaling is limited by its structure. In addition to the complex design structure above, the VECSEL with a simple quantum well (QW) and integrated DBR structure in the folded cavity currently report output power above 10 watts and tuning ranges up to 45 nm. VECSEL with a simpler linear cavity also obtained good results. Although there are many reports of tuning QW VECSEL, the specific theoretical design and experiment reports of wide tuning and high power VECSEL are few. In the report [27], the Double-Band Mirror (DBM) is used to replace DBR to obtain a wider reflection bandwidth, and two InGaAs quantum wells with different Indium compositions to expand the material gain, but this is the theoretical calculation and the experimental results have not been obtained. In another report, the broadband performance VECSEL was obtained by using double well quantum wells and antiresonance structures, and finally, only 43 nm and 2.6 W output were obtained [25]. Therefore, it is of great significance to study the simulation design and experimental verification of wide tuning and high-power VECSEL. Here we simulation designed and demonstrated a temperature-stable, wide-tuned, high-power VECSEL with a simple linear cavity. As a result of the proof-of-concept experiment, a continuously adjustable range of 47 nm, 8 W of output power, and temperature-stable operation were obtained, which verified the feasibility of the design. For the first time, to the best of our knowledge, the tuning such result of VECSEL in the linear cavity is designed and obtained. The experimental results provide a reference value for the design, and experiment of the wide-tuned, high-power, and temperature-stable VECSEL, which can guide the optimization work in the next step.

## II. DEVICE STRUCTURE

The device structure of tunable 1064 nm VECSEL is illustrated in Fig. 2. It consists of a heatsink, gain chip, external output mirror, and pump system. At the bottom of the gain chip is the DBR with high reflectivity, which consists of 25 pairs of quarter-wavelength AlAs/GaAs layers. The active region consists of 14 pairs of InGaAs/GaAs multi-quantum wells (MQWs) sandwiched between two GaAsP strain compensation layers. While the anti-resonant periodic gain structure of VECSEL allows a wider tuning range, high power output is certainly achieved using the resonant periodic gain (RPG) structure. Therefore, in this paper, the RPG structure is still chosen and the quantum well is positioned at the antinode of the cavity standing wave to provide high gain in the active region. Also, for a wide tuning range, the  $\text{Ta}_2\text{O}_5/\text{SiO}_2$  antireflection (AR) layer is coated on the surface of the gain chip to eliminate the effect of microcavity resonance. The pump system consists of an 808 nm, 50 W, fiber-coupled diode bar, emitting from a 100  $\mu\text{m}$  diameter, numerical aperture  $\text{NA} = 0.22$  fiber, and a collimating and focusing lens to image the fiber output onto the VECSEL gain chip. The high-reflectivity DBR at the end of the gain chip and the external output coupling mirror (OC) form a

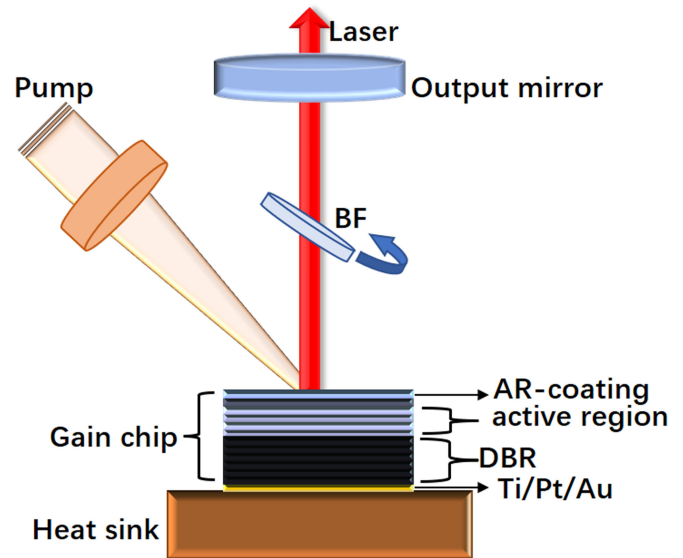


Fig. 2. Schematic diagram of a tunable VECSEL with BF.

simple linear cavity. The radius of the OC is 20 mm, and the cavity length is 17 mm. Finally, a BF is inserted in the simple linear cavity at the Brewster angle to tune the resonant mode of the VECSEL.

## III. DESIGN OF VECSEL CHIP AND CALCULATION OF THE BF

Before the tunable 1064 nm VECSEL epitaxial growth and fabrication, the VECSEL structure must be optimized. The QWs are critical for the VECSEL, which directly determine the threshold, efficiency, and output power of the laser. To obtain a temperature-stabilized, wide-tunable, and high-power VECSEL, the material gain curve of QWs needs to be widely and large, and the thermal performance of QWs needs to be good as possible. In this work, the structure is simulated using the self-consistent modeling software PIC3D. Fig. 3(a) shows the gain spectrum of the InGaAs QWs with different thicknesses at the peak wavelength of 1064 nm. It can be seen that the spectra vary considerably with the thickness of QW and Indium compositions. The peak spectral intensity of QW decreases with increasing thickness except for the 3 nm QW. The low gain peak of the 3 nm QW is due to the too high indium composition (50.8%), which leads to the appearance of lattice mismatch and defects in the InGaAs/GaAs layer. It can also be seen that when the QW thickness exceeds 8 nm, a secondary gain peak appears on the left side of the gain spectrum. This is because the QW energy level splitting effect gets weaker with the increasing thickness, and the separation of the first and second sub-band is insufficient, resulting in the simultaneous emission of both energy levels. The second sub-level has a large band-gap, hence the short gain peak wavelength appears. In addition, the spectral width increases with the thickness of the QW. A wide spectrum will directly benefit the output of a wide tuning range. Therefore, we believe that the spectral width and gain intensity of the QW thicknesses of 7 nm and 8 nm satisfy the design of wide-tuning and high-power output. Fig. 3(b) shows the gain spectrum with

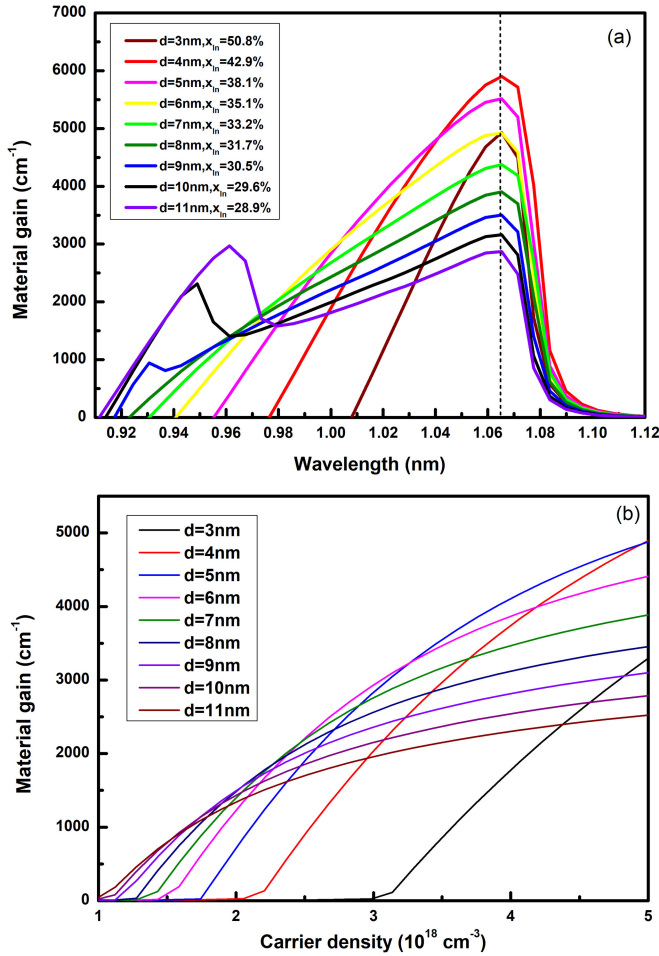


Fig. 3. Fixed Gain peak wavelength at 1064 nm. (a) Comparison spectral of InGaAs quantum wells with different well thicknesses. (b) InGaAs quantum wells gain change with carrier density.

the carrier density, which can represent the gain behavior of the QWs in the actual operation. It can be seen that the performance of 3 nm QWs is still not good, and the 8 nm QW peak gain decrease too much than the 7 nm QWs when the carrier intensity is  $5 \times 10^{18} \text{ cm}^{-3}$ . Finally, for wide-tuned output, a QWs with a thickness of 7 nm is designed to realize tunable 1064 nm VECSEL, and the Full Width at Half Maximum (FWHM) of the spectrum is 85 nm.

In addition to a wide tuning range, it is extremely important that the laser can operate stably over a wide temperature range. Due to self-generated thermal effects, the temperature of the active region in a VECSEL is higher than that of the rest of the gain chip, resulting in wavelength shift and variation of the gain density. Therefore, knowing the trend of the active region with temperature is a beneficial for the design and growth of the VECSEL gain chip. Fig. 4(a) is the Spontaneous Emission Rate (SER) of 7 nm QW with temperature, the peak wavelength of gain is redshifted with the rise of the temperature, and the average speed of redshift is about 0.41 nm/K. The practical wavelength of VECSEL with thermal effect can be calculated based on this speed. Fig. 4(b) shows the peak wavelength (green) and peak gain (blue) with temperature in detail. The peak value of SER

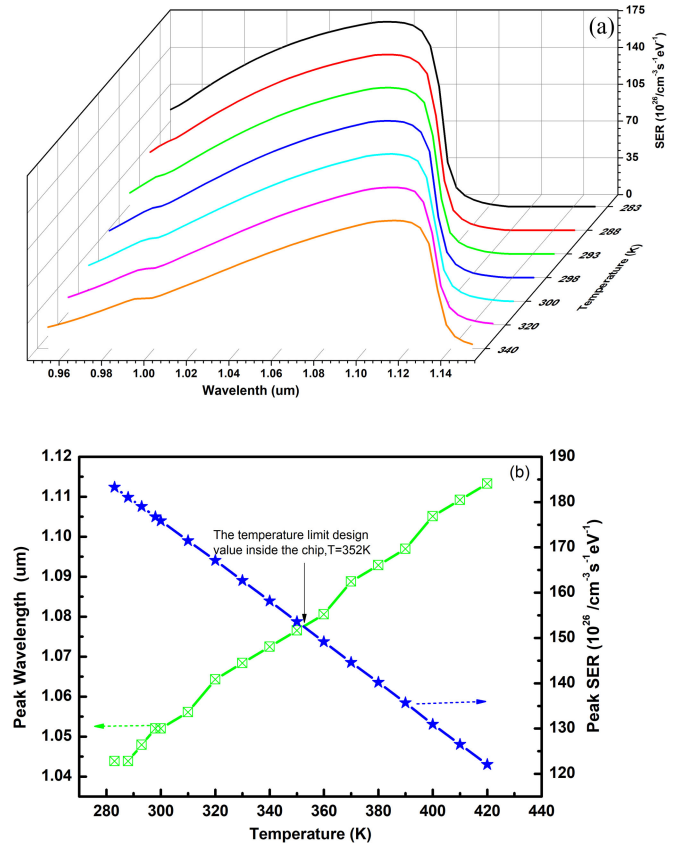


Fig. 4. (a) The spontaneous emission rate (SER) versus wavelength of InGaAs QW at different temperature. (b) The peak wavelength and peak SER versus temperature.

decreases with the rise of the temperature at the velocity of  $0.45 \times 10^{26} / \text{cm}^{-3} \text{ s}^{-1} \text{ eV}^{-1} \text{ K}^{-1}$ . Consequently, the temperature rise of the active region should be controlled well to get a high gain and wavelength cover for 1064 nm at the same time. We believe that the temperature in the active region should not exceed 352 k which can guarantee high gain intensity and correct wavelength. This temperature has important guiding significance for our subsequent thermal management of VECSEL.

In this experiment, a BF is designed to select the lasing wavelength in the VECSEL. The tuning curve of BF is calculated, and the thickness of BF is optimized. The material of BF is the quartz crystal, which is processed into an optical axis C parallel to its surface and is placed in the resonator at a Brewster angle  $\theta_B$ . Thus, the light incident on the BF can be considered as s-polarized light. Due to the birefringent effect of quartz crystal, the linearly polarized light is decomposed into ordinary and extraordinary rays. The transmission matrix of BF can be expressed as

$$T = \begin{pmatrix} \frac{2n^2}{1+n^2} & 0 \\ 0 & n \end{pmatrix} \begin{pmatrix} \cos \theta & -\sin \theta \\ \sin \theta & \cos \theta \end{pmatrix} \begin{pmatrix} 1 & 0 \\ 0 & e^{-i\delta} \end{pmatrix} \\ \times \begin{pmatrix} \cos \theta & \sin \theta \\ -\sin \theta & \cos \theta \end{pmatrix} \begin{pmatrix} \frac{2}{1+n^2} & 0 \\ 0 & 1/n \end{pmatrix}$$

Where  $\theta$  is the angle between the incident wave vector and optical axis C,  $n$  is the average index, and  $\delta$  is the phase delay

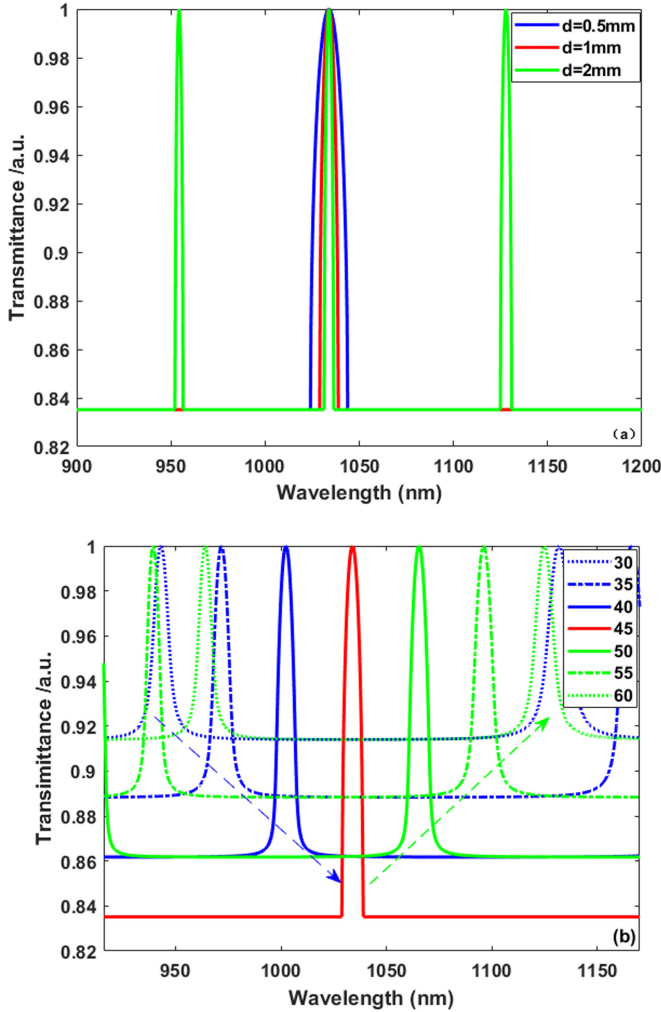


Fig. 5. The transmittance of BF with wavelength (a) different thickness (b)  $\theta$  from  $30^\circ$  to  $60^\circ$ .

between the ordinary and extraordinary ray. Since the polarization of the lasing signal beam should be one of the eigenvectors of the Jones matrix  $T(\theta)$ , we solve for max eigenvectors (normal modes) of  $T(\theta)$  to find the transmittance of the BF. The transmission of BF with different thicknesses is simulated to optimize the tuning range, as shown in Fig. 5(a). The FWHM and the Free Spectral Range (FSR) of the transmission peak of BF increase with wavelength. The 2 mm thickness BF has an FSR of about 80 nm, which is close to the FWHM of the gain spectrum, the 1 mm BF has an FSR of about 149 nm which is sufficient to cover the chip gain width. The 0.5 mm BF can also meet the requirement, but it is too thin and fragile for practical application. A 1 mm thick BF was finally chosen as the tuning element for this experiment. The transmission change with the incident angle  $\theta$  is calculated as shown in Fig. 5(b). Considering the geometric symmetry, the range of  $\theta$  is changed from  $30^\circ$  to  $60^\circ$ . It can be seen from the figure that the transmission wavelength of BF shifts toward longer wavelengths as the angle increases, and the tuning of BF is also periodic with the change of  $\theta$ . The maximum transmittance range and the narrowest curve is the  $\theta$  of  $45^\circ$ , this is because of the s-polarization and p-polarization

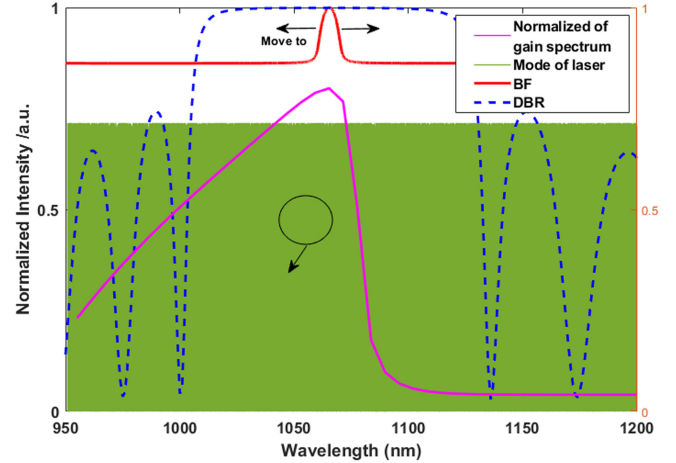


Fig. 6. Simulation of mode distribution when BF is placed in VECSEL.

equipartition at this angle. In the end, we think the tuning range of the 1 mm BF is up to 149 nm around the designed 1  $\mu\text{m}$  wavelength.

Fig. 6 is the simulation of mode distribution when BF is placed in VECSEL. The magenta line is the normalized gain curve with FWHM of 85 nm, the blue dash is the reflection of DBR with 120 nm bandwidth, the red line is the transmission curve of BF with a tuning range of 100 nm at  $45^\circ$ , and the green line is the laser modes in the Fabry-Perot cavity of VECSEL, the inset shows the details of the cavity mode. Changing the angle of incidence  $\theta$ , the transmission peak of the BF moves to other wavelengths within the gain spectrum and the reflection spectrum of the DBR, and the tuning of the laser is achieved. Usually, in practice, the redshift speed of the gain peak is faster than the DBR reflection due to temperature rise, thus the gain peak is designed at the left of the DBR center to obtain a wider tuning range. Finally, a 7 nm InGaAs QW with 85 nm FWHM and 1 mm BF is designed to realize the tunable 1064 nm VECSEL, the temperature is considered not over 352 K inside the gain chip during the thermal management process, and the tuning range of design is about 85 nm.

#### IV. EXPERIMENT AND RESULTS

The gain chip is grown using metal-organic chemical vapor deposition (MOCVD) in an upside-down configure. The grown gain chip is soldered with indium onto a 7 mm \* 7 mm chemical vapor deposition (CVD) diamond heat spreader. After In-soldering on the heatsink, the GaAs substrate is chemically removed to ensure the temperature range in the active region. Finally, the chip is mounted on a copper connected to a thermoelectric cooling (TEC) that can control the temperature on purpose, and the heat of the TEC is taken away by circulating water cooling. Fig. 7 is the output power of the VECSEL with pump current increasing at different heatsink temperatures, and the transmittance of output mirrors is 2%. It can be seen that the laser output power increases linearly with the rise of the pump current. The pump current is up to 4.5 A (power 36 W), and the VECSEL does not appear to be the thermal rollover.

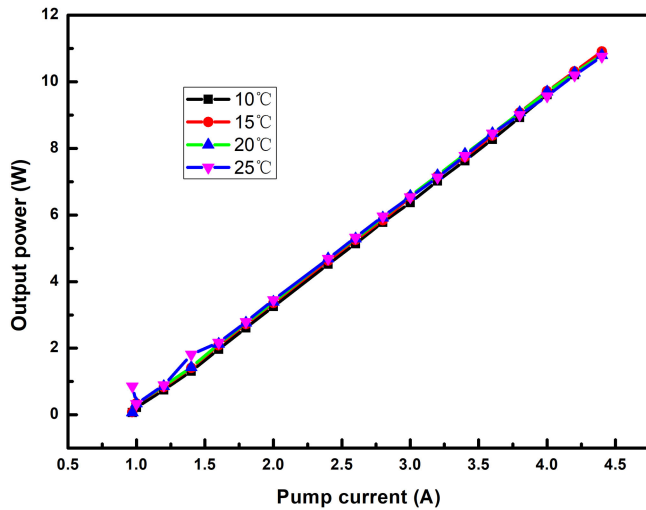


Fig. 7. The output power with the pump current of VECSEL.

When changing the temperature of the heatsink, the output power of the VECSEL still fluctuates slightly and remains almost unchanged at the same pump current. We think this can represent the good thermal management of our VECSEL, the temperature of the QW is controlled below our simulation value of 352 K. For the safety of the chip, the pump current is not increasing continuously, and the maximum power of the VECSEL reaches 11 W at 25 °C. The pump light-laser absorption conversion efficiency is about 43.6%.

Fig. 8 is the partial spectrum of tuning VECSEL. Fig. 8(a) shows the tuning range of VECSEL with the different heatsink temperatures at pump current 3.5 A. It can be seen that the maximum tuning range of the VECSEL is 47 nm at 20 °C, but the range has reduced to 45 nm when changing the temperature range to 10 °C. That means too low or too high a temperature will reduce the tuning range of VECSEL. We think that the temperature rises or drops of 10 °C have the same tuning range caused by completely different reasons. The temperature rises of 10 °C results in a redshift of the gain spectrum with the decrease of density, so the tuning range is narrower than before. On the contrary, decreasing the temperature will lead to the blue shift of wavelength and higher gain, but with new problems. That is, the blue shift will make the gain spectrum located at the edge of the DBR reflection spectrum. The increase in gain density cannot compensate for the loss caused by the decrease of DBR reflectance at this location, so the tuning range is reduced. However, it is worth noting that the entire tuning range changes only a few nm over a wide range of temperatures, which benefits from the good thermal management of the gain chip. Fig. 8(b) is the partial spectrum of tuning VECSEL and the output power at the optimal temperature of 20 °C. The stars represent the output power corresponding to the different tuned wavelengths, and the colored lines represent the partially tuned spectrum. The tuning wavelength of the VECSEL cover from 1044 nm to 1092 nm, and most of the tuned wavelength output power is at the watt level, the maximum output power is 8 W.

As mentioned earlier, the small reduction in temperature leads to a lower tuning range, which indicates that the gain peak design

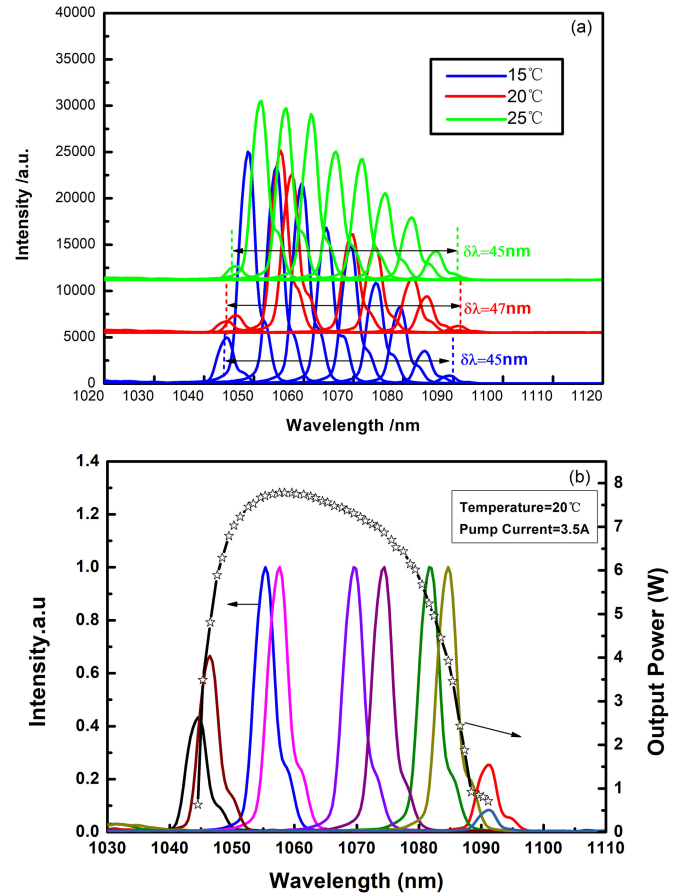


Fig. 8. (a) The partial tuning spectrum of VECSEL at different temperature (b) the output power with pump current 3.5 A at the optimal temperature of 20 °C.

position is consistent with the expected design. But the maximum tuning range is 47 nm is far less than the design range of 85 nm. We attributed this to the limitation of the DBR reflection bandwidth firstly. The higher transmittance can compensate for cavity loss caused by the decreased reflection of DBR. To verify our point of view, output mirrors with different transmittance are used to measure the tuning range under different pump currents, as shown in Fig. 9. The transmittance ( $T$ ) of the OC is 0.1%, 2%, and 3%, and the heatsink is 20 °C. It can be seen from the figure that all the center wavelengths redshift with the increase in the pump current. The maximum tuning range of high reflection mirrors in Fig. 9(a) can reach 46 nm at 3 A, 2% OC in Fig. 9(b) is slightly larger, it can reach 47 nm at 3.5 A, but 3% OC in Fig. 9(c) is reduced to 40 nm at 3 A. The greater transmittance means more loss of cavity, so the tuning range of 3% OC is less than 2% OC. The tuning range of 0.1% OC is lower than that of 2% OC because the 0.1% OC tuning range has not yet reached a maximum at the pump current is 3 A. For the safety of the chip, we did not let the VECSEL with a 0.1% high mirror work at a high pump current for a long time, the data has not been measured. However, in the actual experiment, it can reach the maximum value of 47 nm at the pump current of 3.2 A, and the thermal inversion when the current continues to increase. Subsequently, the maximum tuning range of 2% and

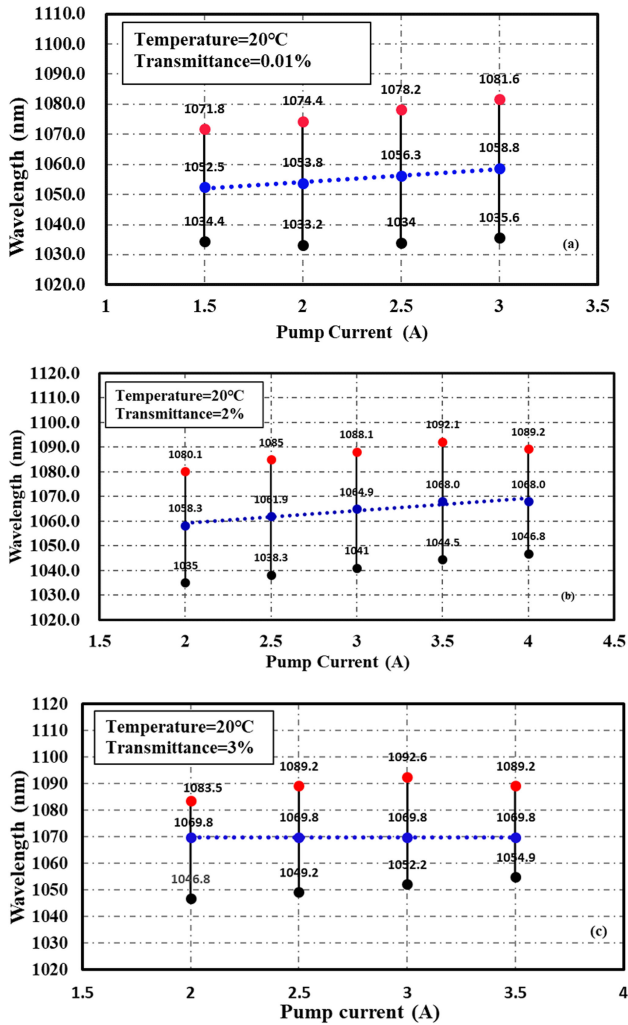


Fig. 9. Tuning range of VECSEL with different transmittance (T) of output mirror. (a) T = 0.01%. (b) T = 2%. (c) T = 3%.

0.1% OC remained at 47 nm with the increase of pump current until thermal inversion. This means that the high reflectivity bandwidth of DBR covers at least 1035 nm to 1092 nm, which is beyond the tuning range of 47 nm that we have achieved. This directly guides us to attribute the restricted tuning range to the lack of gain strength of the QW. Two reasons may cause this, one is the quality of growth is not good, and another is the high gain range of the design is not enough, the gain intensity decreases too quickly with the increasing temperature. The sacrifice of gain also limits the tuning range while ensuring wide tuning in the design. According to the experimental results, in the next step, the peak gain corresponding to the tuning range should be controlled to be greater than  $163 \text{ e}^{26}/\text{cm}^{-3}\text{s}^{-1}\text{eV}^{-1}$ , and the quality of growth needs to be good. This is the important guiding significance for the design and manufacture of the wide tuning VECSEL with stable temperature.

## V. CONCLUSION

We designed and demonstrated a temperature-stable, wide-tuned, high-power VECSEL with a simple linear cavity. Firstly, the gain spectrum of QW and the tuning curve of BF are

simulated to ensure a wide tuning range. The central design wavelength of the gain chip is 1064 nm. Then according to the calculation results, a VECSEL gain chip is fabricated with good thermal management. The surface of the gain chip is coated with an AR layer to eliminate the cavity effects. Finally, a 47 nm tuning range, 8 W of output power, and good thermal performance VECSEL is obtained. This is the first time that such a result has been obtained in a linear cavity QW VECSEL. Although the experimental results are not perfect, we have verified by calculation and experiment that the tuning range of this experiment is limited because the gain intensity of the QW decreases too fast. As a result, the wavelength range with high gain intensity is limited to 47 nm. The results show that the tuning wavelength intensity of spontaneous emission gain intensity should be designed at least higher than  $163 \text{ e}^{26}/\text{cm}^{-3}\text{s}^{-1}\text{eV}^{-1}$ . We call this value the critical gain of wide tuning output, which is important for optimizing wide tuning, temperature stability, and high power VECSEL. As the next step, we plan to design QWs with different structures, materials, and thicknesses based on existing experiments to achieve the maximum width at the critical gain value. We are confident that a tuning range of 80 nm or more can be achieved in a linear QW VECSEL.

## REFERENCES

- [1] E. D. Hinkley and P. L. Kelley, "Detection of air pollutants with tunable diode lasers," *Science*, vol. 171, no. 3972, pp. 635–639, 1971.
- [2] R. N. Zare and P. J. Dagdigan, "Tunable laser fluorescence method for product state analysis," *Science*, vol. 185, no. 4153, pp. 739–747, 1974.
- [3] K. Kawase, "Terahertz imaging for drug detection and large-scale integrated circuit inspection," *Opt. Photon. News*, vol. 15, no. 10, pp. 34–39, 2004.
- [4] T. Chu, N. Fujioka, S. Nakamura, M. Tokushima, and M. Ishizaka, "Compact, low power consumption wavelength tunable laser with silicon photonic-wire waveguide micro-ring resonators," in *Proc. 35th Eur. Conf. Opt. Commun.*, 2009, pp. 1–2.
- [5] Z. Xiaodan, Y. Yibiao, C. Zhihui, W. Yuncai, F. Hongming, and D. Xiao, "Ultra-wide tuning single channel filter based on one-dimensional photonic crystal with an air cavity," *J. Semiconductors*, vol. 38, no. 2, 2017, Art. no. 023004.
- [6] E. Heumann et al., "Semiconductor-laser-pumped high-power upconversion laser," *Appl. Phys. Lett.*, vol. 88, no. 6, 2006, Art. no. 061108.
- [7] O. G. Okhotnikov, *Semiconductor Disk Lasers: Physics and Technology*. Weinheim, Germany: Wiley, 2010.
- [8] E. Kantola, T. Leinonen, S. Ranta, M. Tavast, and M. Guina, "High-efficiency 20 W yellow VECSEL," *Opt. Exp.*, vol. 22, no. 6, pp. 6372–6380, 2014.
- [9] P. Zhang, L. Mao, X. Zhang, T. Wang, L. Wang, and R. Zhu, "Compact dual-wavelength vertical-external-cavity surface-emitting laser with simple elements," *Opt. Exp.*, vol. 29, no. 11, pp. 16572–16583, 2021.
- [10] L. Fan et al., "Extended tunability in a two-chip VECSEL," *IEEE Photon. Technol. Lett.*, vol. 19, no. 8, pp. 544–546, Apr. 2007.
- [11] J. Paajaste, S. Suomalainen, R. Koskinen, A. Härkönen, M. Guina, and M. Pessa, "High-power and broadly tunable GaSb-based optically pumped VECSELs emitting near 2  $\mu\text{m}$ ," *J. Cryst. Growth*, vol. 311, no. 7, pp. 1917–1919, 2009.
- [12] M. Lukowski, C. Henssenius, and M. Fallahi, "Widely tunable high-power two-color VECSELs for new wavelength generation," *IEEE J. Sel. Topics Quantum Electron.*, vol. 21, no. 1, pp. 432–439, Jan./Feb. 2015.
- [13] M. Scheller, T.-L. Wang, B. Kunert, W. Stolz, S. Koch, and J. Moloney, "Passively modelocked VECSEL emitting 682 fs pulses with 5.1 W of average output power," *Electron. Lett.*, vol. 48, no. 10, pp. 588–589, 2012.
- [14] A. Laurain et al., "Modeling and experimental realization of modelocked VECSEL producing high power sub-100 fs pulses," *Appl. Phys. Lett.*, vol. 113, no. 12, 2018, Art. no. 121113.
- [15] L. Fan, "Tunable high-power high-brightness vertical-external-cavity surface-emitting lasers and their applications," Ph.D. dissertation, Univ. Arizona, Tucson, AZ, USA, 2006.

- [16] H. Walther and J. Hall, "Tunable dye laser with narrow spectral output," *Appl. Phys. Lett.*, vol. 17, no. 6, pp. 239–242, 1970.
- [17] Z. Yang, A. R. Albrecht, J. G. Cederberg, and M. Sheik-Bahae, "80 nm tunable DBR-free semiconductor disk laser," *Appl. Phys. Lett.*, vol. 109, no. 2, 2016, Art. no. 022101.
- [18] Z. Yang, A. Albrecht, J. Cederberg, S. Hackett, and M. Sheik-Bahae, *Broadly Tunable DBR-free Semiconductor Disk Laser (SPIE LASE)*. Bellingham, WA, USA: SPIE, 2016.
- [19] A. Broda, A. Wójcik-Jedlińska, I. Sankowska, M. Wasiak, M. Wieckowska, and J. Muszalski, "A 95-nm-wide tunable two-mode vertical external cavity surface-emitting laser," *IEEE Photon. Technol. Lett.*, vol. 29, no. 24, pp. 2215–2218, Dec. 2017.
- [20] H. Kahle, H.-M. Phung, P. Tatar-Mathes, S. Ranta, P. Rajala, and M. Guina, *Membrane External-Cavity Surface-Emitting Lasers (MECSELs) With Broadband Gain in the 9XX to 10XX nm Spectral Range (SPIE OPTO)*. Bellingham, WA, USA: SPIE, 2021.
- [21] M. Butkus et al., "Quantum dot based semiconductor disk lasers for 1–1.3  $\mu\text{m}$ ," *IEEE J. Sel. Topics Quantum Electron.*, vol. 17, no. 6, pp. 1763–1771, Nov./Dec. 2011.
- [22] J. E. Hastie et al., "A 0.5W, 850-nm  $\text{Al}_x\text{Ga}_{1-x}\text{As}$  VECSEL with intracavity silicon carbide heat spreader," in *Proc. 15th Annu. Meeting IEEE Lasers Electro-Opt. Soc.*, 2002, vol. 1, pp. 329–330.
- [23] L. Fan et al., "Tunable high-power high-brightness linearly polarized vertical-external-cavity surface-emitting lasers," *Appl. Phys. Lett.*, vol. 88, no. 2, 2006, Art. no. 021105.
- [24] A. Hein, S. Menzel, and P. Unger, "High-power high-efficiency optically pumped semiconductor disk lasers in the green spectral region with a broad tuning range," *Appl. Phys. Lett.*, vol. 101, no. 11, 2012, Art. no. 111109.
- [25] C. Borgentun, J. Bengtsson, A. Larsson, F. Demaria, A. Hein, and P. Unger, "Optimization of a broadband gain element for a widely tunable high-power semiconductor disk laser," *IEEE Photon. Technol. Lett.*, vol. 22, no. 13, pp. 978–980, Jul. 2010.
- [26] L. Mao, X. Zhang, R. Zhu, T. Wang, L. Wang, and P. Zhang, "Widely tunable external-cavity surface-emitting laser using various methods," *Appl. Opt.*, vol. 60, no. 22, pp. 6706–6712, 2021.
- [27] P. Zhang, M. Jiang, Y. Men, R. Zhu, Y. Liang, and Y. Zhang, "Wafer design of widely tunable vertical-external-cavity surface-emitting laser with broadband gain spectrum," *Opt. Quantum Electron.*, vol. 47, no. 2, pp. 423–431, 2015.